Dielectric spectroscopy of the twist grain boundary phase and smectic-like behaviour in the Isotropic Phase

M. R. Dodge[a]; J. K. Vij[a]; S. J. Cowling[b]; A. W. Hall[b]; J. W. Goodby[b]

[a] Department of Electronic and Electrical Engineering, Trinity College, Dublin 2, Ireland [b] Department of Chemistry, University of York, York YO10 5DD, UK

PLEASE SCROLL DOWN FOR ARTICLE

Dielectric spectroscopy of the twist grain boundary phase and smectic-like behaviour in the Isotropic Phase

M.R. DODGE†, J.K. VIJ*†, S.J. COWLING‡, A.W. HALL‡ and J.W. GOODBY‡

†Department of Electronic and Electrical Engineering, Trinity College, Dublin 2, Ireland
‡Department of Chemistry, University of York, York YO10 5DD, UK

Dielectric properties of a novel liquid crystal with direct transition from isotropic to twist grain boundary (TGB) phase were studied. Measurements were performed over a wide range of temperature in the isotropic phase, TGB_A, TGB_C and SmC^* phases. The Arrhenius plot of the relaxation frequency of the molecular process around the short axis shows a variation in the activation energy in the isotropic phase. This is attributed to smectic-like fluctuations in the isotropic phase. The dielectric relaxation strength in the TGB_C phase has anomalous behaviour in the vicinity of TGB_C–SmC^* transition. The single collective process observed in the TGB_C phase splits into two processes in the SmC^* phase.

1. Introduction

In a seminal work published in 1972, de Gennes pointed out the analogy between the nematic to smectic A transition in liquid crystals and the normal to superconductor transition in metals, and suggested that the incorporation of twist distortion in the smectic A phase could result in a defect-stabilized phase with regular screw dislocations [1]. Based on this analogy Renn and Lubensky developed a mean field theory and predicted that an intermediate phase, which they called twist grain boundary (TGB), could occur between chiral nematic and smectic A [2]. At the same time Goodby *et al.* independently discovered the phase in a highly chiral compound [3]. Further theoretical and experimental investigations led to the discovery of other variants of this phase, namely tilted twist grain boundary phases in the following years [4–9].

Materials with a TGB phase usually have interesting properties at temperatures above the TGB phase. In a large number of TGB compounds, the typical phase sequence may include isotropic, blue phases, chiral nematic, chiral line nematic and $TGB_{(A \text{ or } C)}$ phases [10]. When a nematic phase is not present in the phase sequence, isotropic and TGB phases may be separated by one, two or three smectic blue phases (SmBP) [11]. The symmetries and properties of these phases (SmBPs) have been studied by X-ray, optical and thermal methods [12–16], and it has been found that SmBPIII

is the most stable phase with symmetries similar to those of nematic BPIII, and isotropic phases [14, 16]. The properties of smectic blue phase III are similar to those of the isotropic fog liquid [10], found in a number of compounds including the first TGB material [10, 17]: (i) both phases are optically isotropic; (ii) there are diffuse peaks in the X-ray scattering data of either phase, which suggests the existence of strong smectic-like fluctuations, or a layered structure; (iii) the enthalpy of transition from isotropic to either phase may be quite large and comparable to the enthalpy of transition to the lower temperature TGB phase; (iv) both phases disappear upon racemization.

In this paper we report on a dielectric study of a chiral compound with TGB_A and TGB_C phases, which has strong smectic-like behaviour in the isotropic phase. The phase sequence of the compound is: isotropic–TGB_A–TGB_C–SmC^*. We have included only one isotropic phase in the phase sequence, but our dielectric data suggest the existence of another phase before transition to the TGB phase. This is supported by the X-ray and DSC data [18]. We probe the molecular and collective relaxation phenomena in a wide temperature range in the isotropic, TGB_A, TGB_C and SmC^* phases, and we extract several physical parameters from the experimental data. The Arrhenius plot of relaxation frequency, associated with the rotation around the short axis, indicates that there are two activation energies in the isotropic phase. We attribute this behaviour to the short range smectic-like order in this phase. In addition we report on a collective mode observed in the TGB_A

*Corresponding author. Email: jvij@tcd.ie
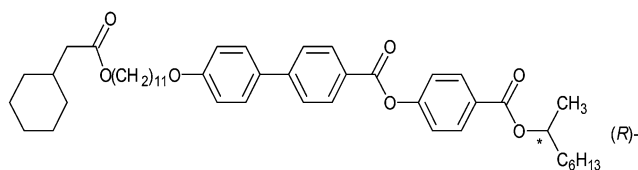
AH29

SmC* 76.1 TGB$_C$ 77.0 TGB$_A$ 78.1 Iso

Figure 1.   Chemical structure of the compound AH29 and its mesogenic phase sequence.

and TGB$_C$ phases. The dielectric relaxation strength associated with this mode has anomalous behaviour on approaching temperature of transition to SmC* phase, and the mode splits into two modes in the SmC* phase.

2.   Experimental

Figure 1 shows the chemical structure of the compound used in this study along with the temperature phase sequence as observed by polarizing optical microscopy, differential scanning calorimetry and X-ray diffraction. Dielectric measurements were carried out in the frequency range 1 Hz–1 GHz using a Novocontrol Dielectric system equipped with an Alpha Dielectric Analyzer (used for 1 Hz–10 MHz measurements) and an Agilent 4291B RF Impedance Analyzer (used for 1 MHz–1 GHz measurements). The high frequency set-up was used mainly to probe the molecular process due to rotation around the long axis. The relaxation frequency range of all other processes, either collective or non-collective mode, is below 4 MHz. For high frequency measurements, a sample cell was made using brass electrodes and a 15 μm Mylar spacer with no alignment layer. For low frequency measurements aligned sample cells, with different thicknesses (1.45, 3.4, 7, 16, 32 μm) were prepared as follows. Indium tin oxide (ITO) coated glass slides with a resistance of 35 $\Omega/\square$ were used for the construction of all cells. Using ITO allowed us to check the alignment of the samples when required. For each cell the ITO coating was etched so as to limit the effective area to a rectangle with typical size of 50–80 mm^2, in the middle of the cell. The slides were cleaned, spincoated with a solution of 0.5 wt % Nylon in methanol, and baked for one hour at 130°C. The glass slides were then unidirectionally rubbed on a velvet cloth, and put together in antiparallel geometry. The sample cells were filled by capillary force in the isotropic phase in a vacuum oven at ~85°C. The temperature of the oven was then lowered to room temperature and the sample

transferred to the dielectric set-up. For each sample, the real and imaginary parts of the complex dielectric permittivity ($\varepsilon' - i\varepsilon''$) were recorded as functions of frequency and temperature, starting from the highest temperature (100°C) in the isotropic phase and cooling the sample slowly to mesogenic phases. The temperature of the sample was adjusted by a flow of dry air at the appropriate, elevated temperature. Temperature steps during the experiment varied from 0.03°C, in the vicinity of transition temperatures, to 1°C far into isotropic or smectic C* phase. An alternating voltage of 0.25 V was used for all dielectric measurements. All measurements were first carried out with no d.c. bias field. In some samples d.c. bias field up to 5 V μm^{-1} was used, but no considerable change in the dielectric properties of the isotropic and TGB phases was observed.

3.   Results and discussion

Figure 2 shows the plot of ε'' for a 7 μm sample as a function of temperature and frequency. The qualitative behaviour of 7 μm and thicker cells was the same. For thinner cells (1.45 and 3.4 μm) the relaxation strength of the processes in the isotropic and TGB phases was very small in comparison with the process due to ITO coating, and in consequence we could not achieve fitting parameters with small errors. In what follows we report the data only for the 7 μm cell unless stated otherwise [There is a slight change in the transition temperatures when using different systems of cell thickner.] The temperature range of the TGB phases is influenced by the thickness of the cell; for the 7 μm cell we observe suppression of this phase by 0.3°C.

A WINFIT software package from Novocontrol Technologies was used for fitting the dielectric loss spectrum to the Havriliak–Negami equation

$$\varepsilon^*(\omega) = \varepsilon_\infty + \sum_{j=1}^{n} \frac{\Delta\varepsilon_j}{\left[1 + \left(i\omega\tau_j\right)^{\alpha_j}\right]^{\beta_j}} + \frac{\Delta\varepsilon_E}{1 + i\omega\tau_E} + \frac{\sigma}{i\varepsilon_0\omega}$$

where ε_∞ is the dielectric permittivity at very high frequency, j is a dummy index corresponding to the j-th relaxation process, n is the number of relaxation processes, which is either one or two, $\Delta\varepsilon = \varepsilon(\omega=0) - \varepsilon_\infty$ is the relaxation strength, τ is the relaxation time, α is the symmetry distribution parameter, and β is an asymmetry parameter. We have included the relaxation process of the ITO electrodes in a separate term (the third term). This process is Debye type and is temperature independent. When the data for this process are fit to the Havriliak–Negami equation we obtain values very close to 1 for the the exponents, and an almost a constant value for the relaxation time with
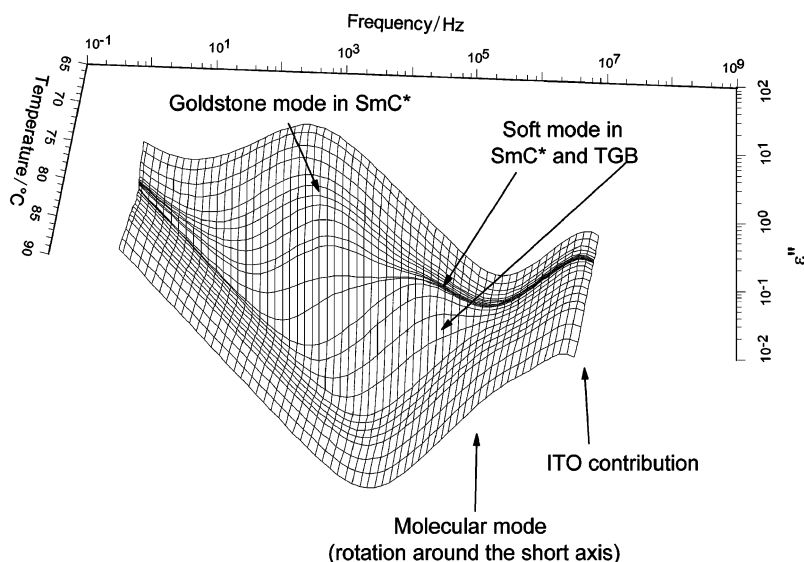
Figure 2. Dielectric loss as a function of temperature and frequency. For clarity of the picture many experimental points are excluded from the graph.

temperature. All parameters in this case have only small variations with temperature. The last term in the expression is the contribution of the conductivity, which is reflected in measurements at low frequencies.

Figure 3 shows the relaxation frequency of all observed processes as a function of temperature. In the high frequency region (above 10 MHz) the only relaxation process observed in this study is due to the molecular rotation around the long axis. As can be seen

on the semi-log plot presented in the figure 3, the relaxation frequency of this process uniformly decreases in the isotropic phase, and transitions to TGB phases and then the SmC* phase do not induce a noticeable change in this behaviour. The collective processes due to fluctuations of polar tilt angle and/or azimuthal angle in the mesogenic phases have no appreciable effect in this frequency range. On the other hand there is a clear change in the relaxation frequency in transition to
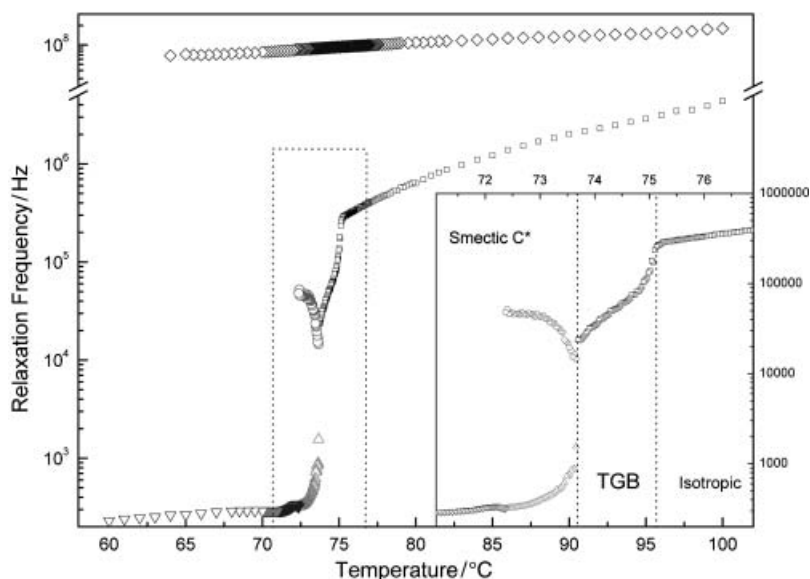

Figure 3. Relaxation frequency of all observed processes versus temperature. The inset is an enlarged version of a 6°C wide temperature region, which includes isotropic, TGB and SmC*.

mesogenic phases in the low frequency data. Several distinct regions, shown in the plot, exist in this frequency region. At high temperatures in the isotropic phase the only observed relaxation process is due to the molecular rotation around the short axis. Transition to the TGB$_A$ phase hinders this rotation, and the appearance of collective modes with very high relaxation strengths makes it impossible to probe this process in the TGB$_A$, TGB$_C$ and SmC* phases. The behaviour of the relaxation frequency of this process in the isotropic phase is different from that of the high frequency region. There is a negative curvature in the semi-log plot of the relaxation frequency versus temperature. This curvature is not an artefact. It was observed in all cells, including the cell with brass electrodes and no alignment layer.

In figure 4 we have plotted the relaxation frequency versus inverse temperature. In the isotropic phase of a liquid crystal the logarithm of the relaxation frequency varies linearly with respect to inverse temperature with small deviations from linearity in the vicinity of the isotropic–mesogenic phase transition. The slope of the curve gives the activation energy. The change of slope corresponds to a change in activation energy, which could be due to a variation in the degree of order and/or the local viscosity [19]. Using Debye theory of dielectric

dispersion the viscosity associated with the rotation of the molecules around the short axis may be written as $\gamma = kT/(8\pi^2 f_c l^3)$, where k is the Boltzmann constant, f_c is the relaxation frequency and l is the length of the molecule [20]. Ignoring all the constants including the molecular length, we calculate the viscosity in an arbitrary unit; the result is shown in the inset of figure 4. There are clearly two regions in the isotropic phase. Considering the fact that in Debye theory the smectic interaction is not considered, a more realistic model would give a sharper change in the viscosity. Arrhenius plots of both relaxation frequency and viscosity are consistent with the X-ray scattering data, which suggest that the lamellar structure of the TGB phase does not completely disappear in transition to the isotropic phase. Figures 5(*a*) and 5(*b*) show the X-ray scattering data and the calculated layer thickness as a function of temperature for this compound.

Formation of a layered structure with short range interaction in the isotropic phase should be accompanied by an unusual increase in the density upon cooling. An increase in density, in general, hinders the molecular rotation, both around the long and the short axes, and results in longer relaxation time or smaller relaxation frequency, as can be seen in the high temperature region
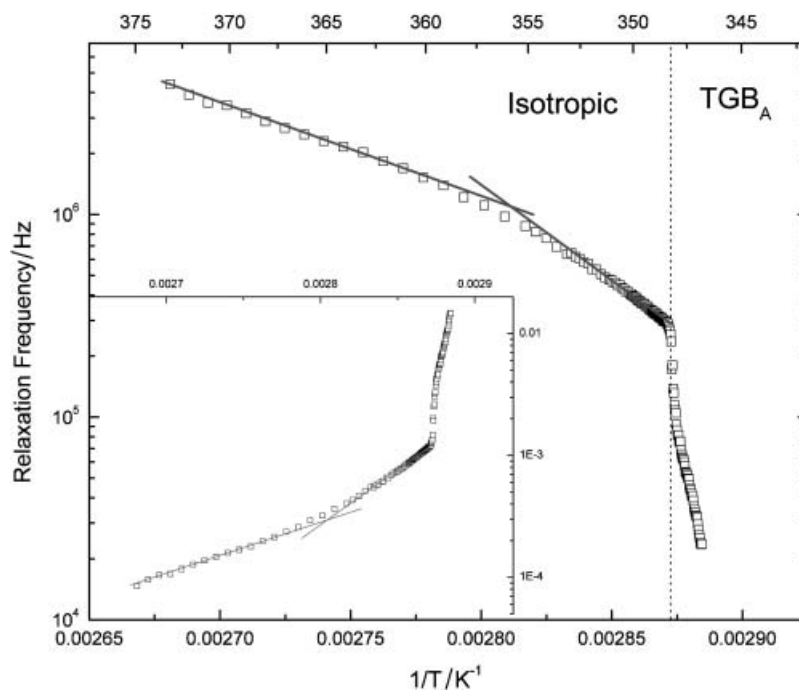

Figure 4. Arrhenius plot of relaxation frequency versus inverse temperature (main graph). The upper scale is temperature in Kelvin, and plotted in reciprocal scale. The inset is the Arrhenius plot of the viscosity of rotation around the short axis in the isotropic phase, in arbitrary units versus inverse temperature.
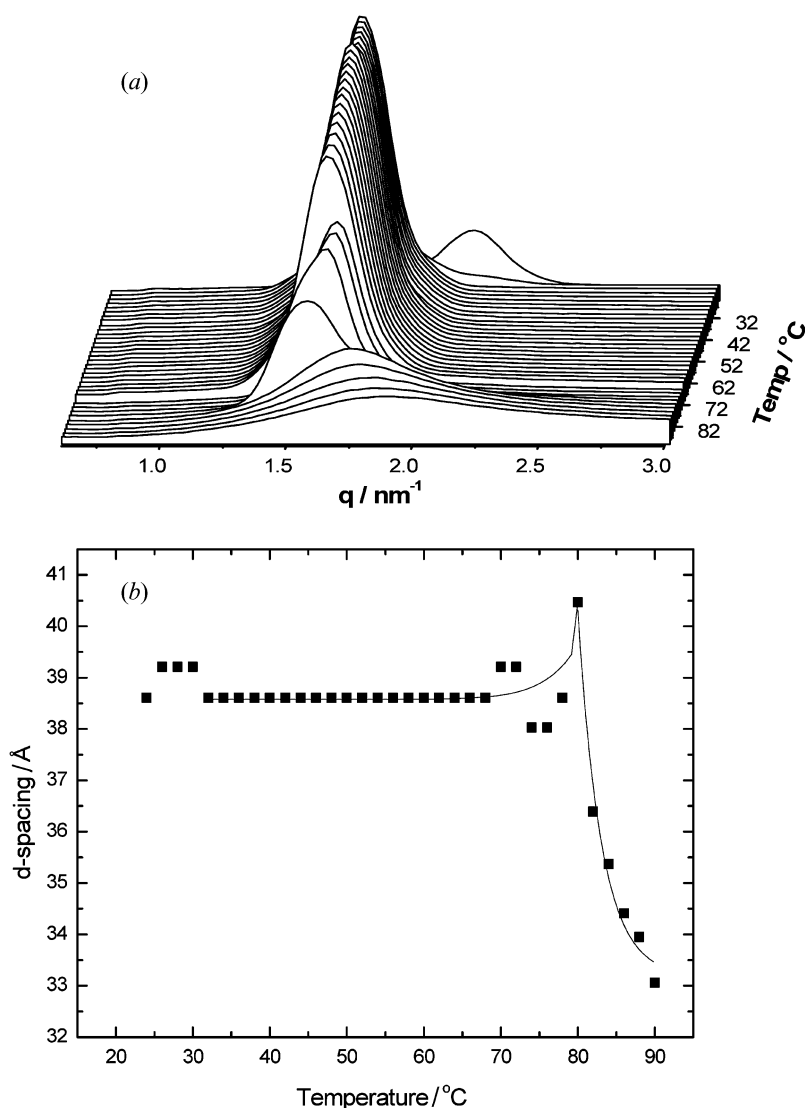
Figure 5. (*a*) X-ray scattering data as a function of wavenumber. (*b*) Layer thickness of the lamellar structure of the compound AH29 as a function of temperature.

of figure 3. Molecular rotation around the long axis is not usually influenced by layer formation, even on transition from the isotropic to a mesogenic phase [21, 22]. This means that the behaviour of the high frequency data is not expected to change by the appearance of such a short range interaction. On the other hand this ordering hinders the molecular rotation around the short axis to a larger extent, and in consequence the relaxation frequency decreases at a faster rate with a decrease in temperature (figure 3) than without the layered structure.

We now turn to the dielectric properties in the TGB and SmC* phases. The molecular processes are not detectable in these phases where the other dominant modes are present. This is because the collective relaxation processes observed in these phases have very high dielectric relaxation strengths in comparison with the relaxation strength of the molecular processes. The relaxation strength of the low frequency phenomena is shown in figure 6 (*a*). The strength is nearly uniform in the isotropic phase. There is a pretransitional effect, which can be seen clearly in the plot of the reciprocal of the relaxation strength in figure 7 (*a*). This slight decrease in the relaxation strength may be attributed to the dipole pairings in the smectic-like behaviour in the isotropic phase. As can be seen in figures 3, 6 and 7 the TGB$_A$–TGB$_C$ transition is not easily observable in the dielectric data. This transition appears as a slight change in the slope of the reciprocal of the relaxation strength versus temperature. The slope
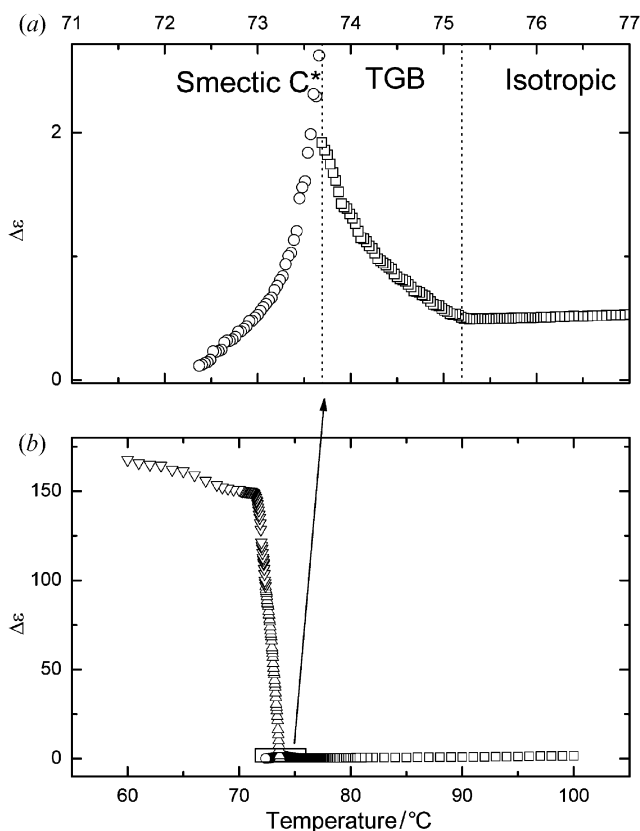
Figure 6.   Dielectric relaxation strength of different processes. (*a*) The enlarged view of the rectangle shown in (*b*).

Figure 7.   (*a*) Inverse of the dielectric relaxation strength for different processes. (*b*) The rectangle area in plot (a) has been enlarged in to present the behaviour of the data in the vicinity of the transition temperatures.

decreases from $1.1°C^{-1}$ in the TGB_A to $0.8°C^{-1}$ in the TGB_C. A similar observation has been reported by Ismaili *et al.* [23].

The behaviour of dielectric parameters in the TGB phases resembles a soft mode in smectic A*: (i) the relaxation frequency in the vicinity of the transition temperature decreases linearly with respect to temperature on a semi-log plot (figure 3), (ii) the dielectric relaxation strength increases to a maximum at the transition temperature, figure 6(*b*), (iii) the reciprocal of the relaxation strength linearly decreases with temperature, figure 7(*b*), (iv) the mode splits into Goldstone and soft mode in the SmC*, figures 3, 6(*b*), 7(*b*). Such behavior is expected in the transition from SmA* to SmC*. In both SmA* and SmC* phases the fluctuations of the amplitude of polarization, or the polar angle θ, give rise to the soft mode, which can be detected in the vicinity of the transition temperature [24]. We do not intend to address this issue in this paper but expect to cover it in a future publication.

To summarize, using dielectric spectroscopy we have investigated a liquid crystal with direct transition from isotropic to TGB_A phase over a broad range of temperature. The Arrhenius plots of the relaxation
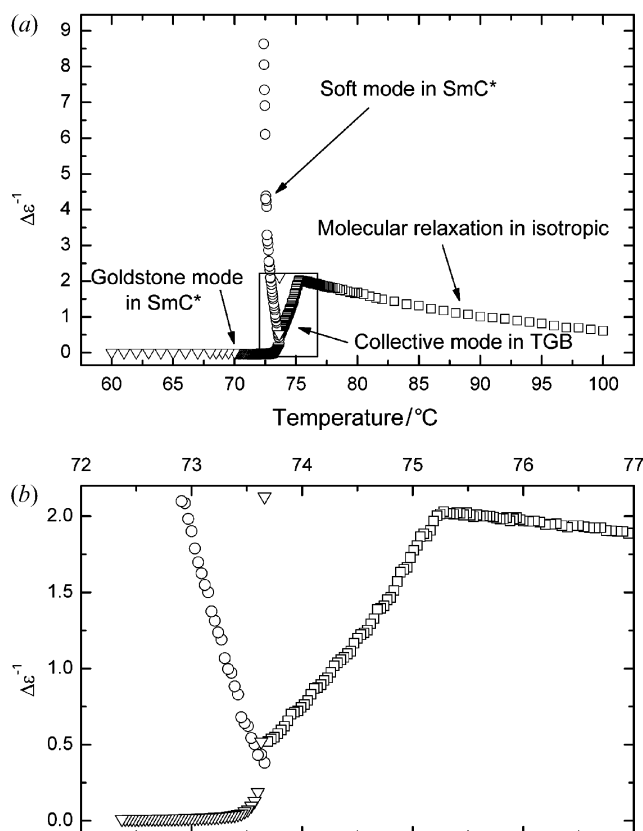
frequency and the rotational viscosity show two distinct regions in the isotropic phase. Combining the dielectric data with X-ray scattering data in which there are diffuse peaks in the isotropic phase, we attribute this behavior to a smectic-like order above the transition to the TGB_A phase. Our dielectric data for the TGB phase show that there is a collective process in the TGB_C phase. The relaxation strength of this process increases to a maximum at the transition to the SmC* phase, where the process splits into two, namely soft mode and Goldstone mode, in the SmC*.

Acknowledgements

References

[1] P.G. de Gennes. *Solid State Commum.*, **10**, 753 (1972).
[2] S.R. Renn, T.C. Lubensky. *Phys. Rev. A*, **38**, 2132 (1988).

[3] J.W. Goodby, M.A. Waugh, S.M. Stein, E. Chin, R. Pindak, J.S. Patel. *Nature*, **337**, 449 (1989).

[4] S.R. Renn, T.C. Lubensky. *Mol. Cryst. liq. Cryst.*, **209**, 349 (1991).

[5] S.R. Renn. *Phys. Rev. A*, **45**, 953 (1992).

[6] H.T. Nguyen, A. Bouchta, L. Navailles, P. Barois, N. Isaert, R.J. Twieg, A. Maanoufi, C. Destrade. *J. Phys. II (Fr.)*, **2**, 1889 (1992).

[7] L. Navailles, P. Barois, H.T. Nguyen. *Phys. Rev. Lett.*, **71**, 545 (1993).

[8] P.A. Pramod, R. Pratibha, N.V. Madhusudana. *Curr. Sci.*, **73**, 761 (1997).

[9] J.W. Goodby, A. Petrenko, M. Hird, R.A. Lewis, J. Meier, J.C. Jones. *Chem. Commum.*, **13**, 1149 (2000); J.G. Meier, P. Rudquist, A.S. Petrenko, J.W. Goodby, S.T. Lagerwall. *Liq. Cryst.*, **29**, 179 (2002).

[10] J.W. Goodby. *Struct. Bond.*, **95**, 83 (1999).

[11] B. Pansu, M.H. Li, H.T. Nguyen. *J. Phys. II (Fr.)*, **7**, 751 (1997).

[12] M.H. Li, V. Laux, H.T. Nguyen, G. Siguad, P. Barois, N. Isaert. *Liq. Cryst.*, **23**, 389 (1997).

[13] B. Pansu, E. Grelet, M.H. Li, H.T. Nguyen. *Phys. Rev. E*, **62**, 658 (2000).

[14] P. Jamee, G. Pitsi, M.H. Li, H.T. Nguyen, G. Siguad, J. Thoen. *Phys. Rev. E*, **62**, 3687 (2000).

[15] E. Grelet, B. Pansu, H.T. Nguyen. *Phys. Rev. E*, **64**, 010703R (2001).

[16] E. Grelet, B. Pansu, M.H. Li, H.T. Nguyen. *Phys. Rev. E*, **65**, 050701R (2002).

[17] J.W. Goodby, M.A. Waugh, S.M. Stein, E. Chin, R. Pindak, J.S. Patel. *J. Am. chem. Soc.*, **111**, 8119 (1989).

[18] S.J. Cowling, A.W. Hall, J.W. Goodby (In preparation).

[19] D. Dunmur, K. Toriyama. In *Physical Properties of Liquid Crystals*, Chap. IV, Sect. 4, Wiley-VCH (1999).

[20] S.T. Lagerwall. *Ferroelectric and Antiferroelectric Liquid Crystals*. Wiley-VCH, Weinheim (1999).

[21] Y.P. Panarin, O. Kalinovskaya, J.K. Vij, J.W. Goodby. *Phys. Rev. E*, **55**, 4345 (1997).

[22] J. Schacht, P. Zugenmaier, M. Buivydas, L. Komitov, B. Stebler, S.T. Lagerwall, F. Gouda, F. Horii. *Phys. Rev. E*, **61**, 3926 (2000).

[23] M. Ismaili, F. Bougrioua, N. Isaert, C. Legrand, H.T. Nguyen. *Phys. Rev. E*, **65**, 011701 (2001).

[24] F. Gouda, K. Skarp, S.T. Lagerwall. *Ferroelectrics*, **113**, 165 (1991).